Universal efficiency and gain computations for high-gain free-electron-laser amplifiers

J. H. Booske
Department of Electrical and Computer Engineering, University of Wisconsin, Madison, Wisconsin 53706

S. W. Bidwell, B. Levush, T. M. Antonsen, Jr., and V. L. Granatstein
Laboratory for Plasma Research, University of Maryland, College Park, Maryland 20742

(Received 4 September 1990; accepted for publication 7 March 1991)

The free-electron-laser (FEL) equations are reduced to a set of one-dimensional, normalized equations that allow a universal (dimensional) analysis. In universal parameters, numerical integration of the FEL equations indicates a relatively constant saturated ponderomotive wave amplitude independent of both the normalized wiggler potential amplitude and the injected signal level. The constant ponderomotive wave amplitude and an empirical fit for the universal saturation length as a function of normalized wiggler potential amplitude and gain permits unnormalized design calculations for saturated power and saturated length over a wide parameter range. Tapering is considered by deriving analytical expressions for the intrinsic efficiency and taper length. Design values for a high-gain, high-efficiency, tapered amplifier at 280 and 560 GHz are presented.

I. INTRODUCTION

It has long been recognized that universal (or dimensional) analyses of dynamic systems provide considerable benefit by reducing the number of free parameters.[1] The result is that considerably larger physical parameter spaces can be studied with more modest and manageable theoretical (or computational) parameter spaces. Consequently, it is not surprising that by reducing the free-electron-laser (FEL) equations of motion to a particularly simple set via convenient parameter definitions and normalizations, it has become possible to perform detailed and extensive simulations on such highly nonliner effects as FEL oscillator efficiency optimization,[2,3] multimode competition and control,[4,5] dynamic oscillator evolution,[6] beam voltage slewing effects,[7] and harmonic generation and competition in FEL amplifiers.[8] In this article we apply the universal normalizations used in the above references to make a few basic observations regarding the general behavior of high-gain[9] FEL amplifiers. We then show how the results of our computations can be used to obtain estimates for the performance characteristics of specific high-gain FELs.

II. FORMULATION

The analysis starts with the equations governing the particle motion (viz., the pendulum equations) and the slowly varying envelope form[10] of the wave equation. Here, we consider the FEL interaction to involve only a single transverse mode at the fundamental FEL frequency (i.e., we neglect harmonics). In addition, since our interest will be in the high-gain (noncollective) regime, we neglect space-charge effects. To obtain a one-dimensional wave equation, we average over the spatial transverse dimensions. With these assumptions, the system equations[3] can be written in the form

$$\frac{d\delta\gamma}{dz}=-2\frac{\omega}{c}\frac{a_w\mathscr{C}}{\gamma_r\bar{\beta}_{zr}}\,\mathrm{Im}(a_s e^{i\psi})-\frac{d\gamma_r}{dz}, \tag{1}$$

$$\frac{d\psi}{dz}=\frac{\omega}{c}\frac{\delta\gamma}{\bar{\beta}_{zr}}\left(\frac{1}{\bar{\beta}_{zr}}\frac{\partial\bar{\beta}_{zr}}{\partial\gamma_r}\right), \tag{2}$$

and

$$\frac{da_s}{dz}=\frac{-i}{2k_z c^2}\frac{4\pi e^2}{m}\frac{gn_b S_b}{S_s}\frac{a_w\mathscr{C}}{\gamma_r}\langle e^{-i\psi}\rangle. \tag{3}$$

In Eqs. (1)–(3), $a_w = eA_w/mc^2$ is the normalized wiggler potential amplitude (or wiggler parameter) and $a_s = eA_s/mc^2$ is the normalized radiation (signal) field amplitude. The period-averaged longitudinal resonant velocity $\bar{\beta}_{zr}$ (normalized to the speed of light c) is defined in terms of the local axial velocity $\beta_z(z)$

$$\bar{\beta}_{zr}\equiv\left(\frac{1}{l_w}\int_0^{l_w}\frac{dz'}{\beta_z(z')}\right)^{-1}, \tag{4}$$

and the resonance condition

$$\omega=(k_w+k_z)c\bar{\beta}_{zr}[z,\gamma_r(z)]. \tag{5}$$

$\gamma_r(z)$ is the resonant value of total energy $\gamma = (1-\beta^2)^{-1/2}$ that is required to keep particles in phase with the ponderomotive wave in the presence of a tapered wiggler, and $\delta\gamma = \gamma - \gamma_r$ is the energy deviation from resonance. The brackets $\langle\ \rangle$ in Eq. (3) represent an average over the initial particle phases in the ponderomotive well. The coupling coefficient $\mathscr{C}$ can be derived generally as[8]

$$\mathscr{C}=\frac{1}{2T}\int_0^T dt\left(e^{i[(k_z+k_w)z-\omega t]}+e^{i[(k_z-k_w)z-\omega t]}\right), \tag{6}$$

where T is the transit time of an electron through one wiggler period. In most problems of interest, however, the condition $a_w^2/(\gamma^2-1)\ll 1$ will justify using the approximate form[11]

$$\mathscr{C}\approx\tfrac{1}{2}[J_0(u_w)-J_1(u_w)], \tag{7a}$$

where

 0021-8979/91/117503-07$03.00

$$u_w = a_w^2/4(1+\tfrac{1}{2}a_w^2), \quad (7b)$$

and J_0, J_1 are the standard Bessel functions.

One quantity of interest is the period-averaged axial energy parameter $\overline{\gamma}_{zr}$. Rigorously, $\overline{\gamma}_{zr} = (1 - \overline{\beta}_{zr}^2)^{-1/2}$ where $\overline{\beta}_{zr}$ is defined in Eq. (4). Functionally, the evaluation of Eq. (4) yields $\overline{\beta}_{zr}$ in terms of a complete elliptic integral:

$$\overline{\beta}_{zr} = \pi\beta_r/2K(\mu) \quad (8a)$$

so that

$$\overline{\gamma}_{zr} = \{1 - [\pi\beta_r/2K(\mu)]^2\}^{-1/2}, \quad (8b)$$

where

$$\mu \equiv a_w^2/\gamma_r^2\beta_r^2 = a_w^2/(\gamma_r^2 - 1). \quad (8c)$$

Further, the exact expression in Eq. (8b) can be approximated, yielding a more familiar form:

$$\overline{\gamma}_{zr} \simeq \gamma_r/\sqrt{1 + a_w^2/2}. \quad (9)$$

This approximate expression is useful when values of μ do not approach unity. Consider a numerical example. Given $\mu = 0.80$ and $\gamma_r = 2.96$ the exact expression Eq. (8b) yields $\overline{\gamma}_{zr} = 1.32$ whereas the approximate expression Eq. (9) gives $\overline{\gamma}_{zr} \simeq 1.46$, an error of 10%.

Finally, in performing the average over transverse dimensions, it has been assumed that the beam waist is much smaller than the radiation waist. This yields the cross-sectional areas for the electron beam S_b and the radiation beam S_s (S_s is the waveguide cross section if relevant), and a normalization factor g for the transverse average of the radiation profile:

$$g^{-1} = \frac{1}{S_s}\int \frac{|a_s(\mathbf{x}_\perp)|^2}{a_s^2}\, d^2\mathbf{x}_\perp \quad (10)$$

where a_s is the peak signal amplitude at $\mathbf{x}_\perp = 0$. The electron-beam density is represented by the symbol n_b. Note that the ratio gS_b/S_s serves as the beam filling factor.

At this point we recognize that the description of an FEL signal-pass amplifier will be most conveniently handled by separate discussion of its two basic sections, as depicted in Fig. 1. Specifically, we expect the amplifier to consist of an initial untapered (uniform wiggler), high-gain region—in which the radiation signal evolves to saturation—followed by a tapered wiggler section for efficiency enhancement. The advantages of such a configuration have been convincingly demonstrated by experiment.[12] Numerical computations using a universal set of equations are particularly well suited to a treatment of the initial high-gain, uniform wiggler region (see Fig. 1). For the tapered section, however, a simple energy balance relation based on Eqs. (1)–(3) above will suffice within the context of the simplified analyses presented here.

III. HIGH-GAIN (UNIFORM WIGGLER) SECTION

In the initial uniform wiggler section, the resonant normalized energy γ_r is constant and the deceleration term

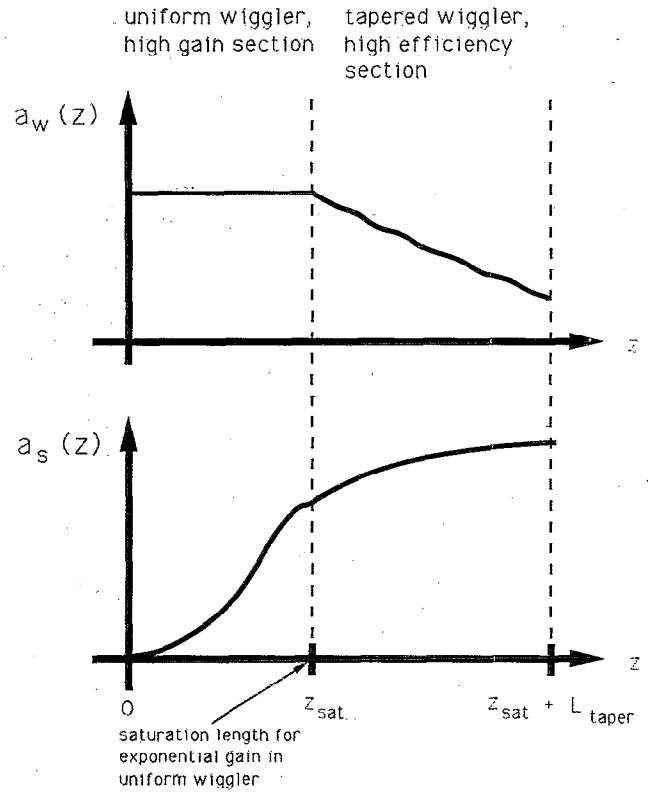

FIG. 1. Tapered FEL amplifier showing wiggler parameter a_w and normalized signal potential a_s with axial distance.

$d\gamma_r/dz$ will not contribute to Eq. (1). We proceed to define the following "universal" quantities:

$$\mathscr{P} \equiv (\omega\mathscr{L}/c)\delta\gamma, \quad (11)$$

$$\mathscr{A} \equiv (\omega\mathscr{L}/c)^2\left(\frac{1}{\overline{\beta}_{zr}}\frac{\partial \ln \overline{\beta}_{zr}}{\partial\gamma_r}\right)^{-1}\frac{a_w a_s}{\gamma_r\overline{\beta}_{zr}}, \quad (12)$$

$$\xi \equiv \left(\frac{1}{\overline{\beta}_{zr}}\frac{\partial \ln \overline{\beta}_{zr}}{\partial\gamma_r}\right)\frac{z}{\mathscr{L}}, \quad (13)$$

and

$$\mathscr{L} \equiv \left[\frac{4\pi g}{S_s}\frac{\overline{I}_z}{I_A}\frac{(\omega/c)^2}{k_z}\left(\frac{a_w}{\gamma_r}\right)^2\left(\frac{\partial \ln \overline{\beta}_{zr}}{\partial\gamma_r}\right)^{-2}\right]^{-1/3}. \quad (14)$$

In Eqs. (11)–(13), the dimensionless quantities $\mathscr{P}$, $\mathscr{A}$, and ξ serve the role of normalized detuning, ponderomotive (or beat) wave amplitude, and longitudinal distance. In Eq. (12), $\mathscr{L}$ is a characteristic length related to the gain length. (Note that $\mathscr{L}$ is not dimensionless.) The two previously undefined current quantities are the period-averaged axial current

$$\overline{I}_z = en_b S_b \overline{\beta}_{zr} c \quad (15a)$$

and

$$I_A = mc^3/e = 1.7\times 10^4 \text{ A}, \quad (15b)$$

which is related to the Alfvén current.

Substituting the quantities defined above into Eqs. (1)–(3), we obtain a universally normalized set of equations for the high-gain section:

$$\frac{d\mathscr{P}}{d\xi} = -2\mathscr{C}\ \mathrm{Im}(\mathscr{A}e^{i\psi}), \tag{16}$$

$$\frac{d\psi}{d\xi} = \mathscr{P}, \tag{17}$$

and

$$\frac{d\mathscr{A}}{d\xi} = \frac{-i\mathscr{C}}{2}\langle e^{-i\psi}\rangle. \tag{18}$$

Note that with proper definition, we could have absorbed the coupling coefficient $\mathscr{C}$ into the universal parameters. Our philosophy, however, was to generate a universal set of computational results which the reader could easily relate to independent FEL configurations by unraveling normalized quantities via Eqs. (11)–(14). Such an exercise is demonstrated later with several quantitative examples. Due to the Bessel function dependence in Eq. (7a), however, inclusion of $\mathscr{C}$ in the universal parameters would have made this unraveling process much more tedious. Hence, we have kept $\mathscr{C}$ out of the normalizations, and vary it explicitly (by varying a_w) as an additional free parameter in the numerical computations.

For the high-gain regime, it is not so important to detune the injection energy from the resonant value. This is particularly true in FELs in which conducting waveguide walls are present to prevent diffraction of radiation away from the electron beam. Hence, here we take the injection value of normalized detuning as equal to zero. Other analyses[13] explore the effects of energy detuning when radiation diffraction and optical guiding are important.

We now numerically solve the nonlinear equation set (16)–(18) for a monoenergetic ensemble of beam electrons. As a result of setting the initial value of detuning to zero, we expect that the evolution of the universal ponderomotive wave amplitude $\mathscr{A}$ will only depend on the initial value $\mathscr{A}_0$ and a secondary weak dependence on a_w through the coupling coefficient. This prediction is verified in the following plots. First, in Fig. 2, we have plotted a typical example of how $\mathscr{A}$ [specifically the natural logarithm $\ln(\mathscr{A}/\mathscr{A}_0)$] evolves with the universal axial coordinate ξ. The onset of exponential growth is evident, as is the inevitable saturation. We can determine from Fig. 2 that in the normalized formulation the exponentiation length has the universal value of approximately $\xi_{\mathrm{exp}} \approx 2.4$. In Fig. 3 we have plotted the wave amplitude at saturation $\mathscr{A}_{\mathrm{sat}}$ as a function of the initial value $\mathscr{A}_0^{-1}$. Note that $\mathscr{A}_{\mathrm{sat}} \approx 0.6$ is essentially independent of $\mathscr{A}_0$, except in the limit that $\mathscr{A}_0 \approx \mathscr{A}_{\mathrm{sat}}$. Figure 4 shows the (universal) saturation length ξ_{sat} versus the power amplification factor $G = (\mathscr{A}_{\mathrm{sat}}/\mathscr{A}_0)^2$ for values of a_w between 0.1 and 5.0. Since $\mathscr{A}_{\mathrm{sat}}$ is essentially constant, this figure is an extremely general characterization of FEL amplifier saturation. Also plotted in Fig. 4 are least-squares fits to the numerical data for $\xi_{\mathrm{sat}}(G,a_w)$. This empirically determined scaling has the approximate form

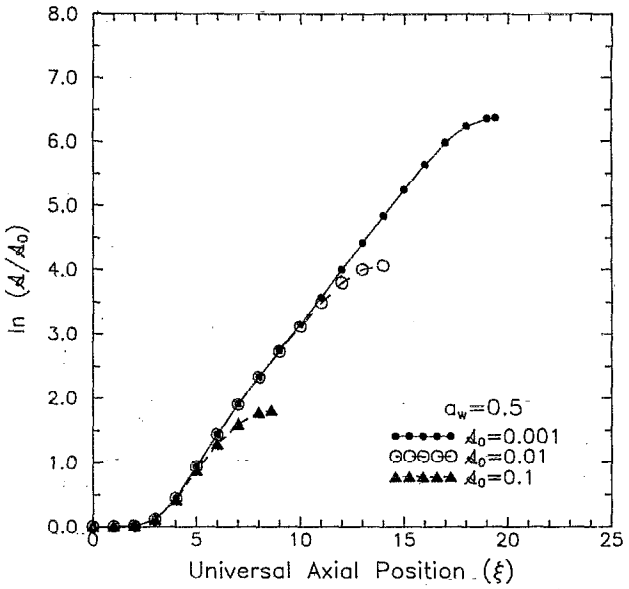

FIG. 2. Growth of ponderomotive amplitude $\mathscr{A}$ with axial distance ξ in uniform wiggler section for case of wiggler parameter $a_w = 0.5$. Three injected amplitudes $\mathscr{A}_0$ are shown.

$$\xi_{\mathrm{sat}}(G,a_w) \approx C_1(a_w)\ln[C_2(a_w)G], \tag{19a}$$

where

$$C_1 \approx 1.05 + 0.117a_w - 0.0114a_w^2 \tag{19b}$$

and

$$C_2 \approx 144 - 30.8a_w + 4.25a_w^2. \tag{19c}$$

At this point we wish to mention that it has recently come to our attention that similar analyses (unpublished) have

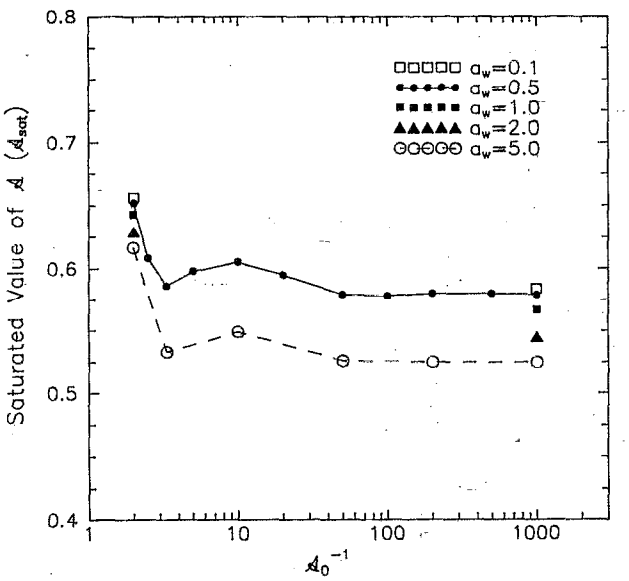

FIG. 3. Saturated ponderomotive amplitude $\mathscr{A}_{\mathrm{sat}}$ with injected amplitude $\mathscr{A}_0$ for five wiggler parameters a_w ranging from 0.1 to 5.0.

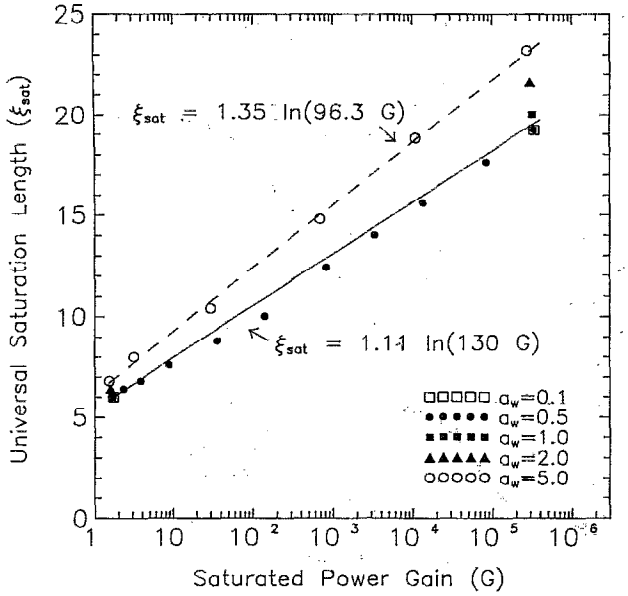

FIG. 4. Universal saturation length ξ_{sat} with saturated power gain G for five wiggler parameters a_w ranging from 0.1 to 5.0. ξ_{sat} is the normalized distance to saturation while power gain $G \equiv P_{sat}/P_0$. The empirical line fits are for $a_w = 0.5$ (solid line) and $a_w = 5.0$ (dashed line) and are calculated from Eqs. (19).

been independently performed by Kumada and Sessler.[14] The results reported here are in good agreement with that work.

These results, obtained by numerical solution of the universal FEL amplifier equations, can be combined with the definitions of the universal parameters to provide a useful, simple method for predicting the behavior of high-gain FELs. For example, following a derivation given in Ref. 3, the saturated signal power is calculated by integrating the axial component of the time-averaged Poynting vector over the transverse waveguide dimensions

$$P = \int d^2\mathbf{x}_\perp \langle \mathbf{S}\cdot\hat{\mathbf{e}}_z\rangle_{\text{time}}, \tag{20a}$$

where the Poynting vector

$$\mathbf{S} = (c/4\pi)(\mathbf{E}\times\mathbf{B}). \tag{20b}$$

With rectangular waveguides and planar wigglers, a common transverse mode for FEL interaction is the TE_{01} mode[3,12,15] which has a one-half sinusoidal variation in the narrow-waveguide dimension and is characterized by a transverse profile average $g = 2$ [see Eq. (10)]. We calculate the saturated power in the TE_{01} mode using Eqs. (20:

$$P_{sat}(TE_{01}) = (\omega k_z/4\pi)(mc^2/e)^2 S_s a_{s,sat}^2, \tag{21}$$

where the saturated normalized signal potential is found simply through Eqs. (12) and (14),

$$a_{s,sat} = (4\pi g e/mc^3)^{2/3} a_w^{1/3} (c/\omega k_z)^{2/3} (\overline{\gamma}_{zr}\overline{\beta}_{zr})^{2/3} \times (\overline{I}_z/S_s)^{2/3} \mathscr{A}_{sat}. \tag{22}$$

Substitution of Eq. (22) into Eq. (21) yields a useful expression for saturated power in terms of the universal saturated ponderomotive amplitude:

$$P_{sat}(TE_{01}) = [(64\pi)(1/\omega k_z) \times (mc^2/e)^2 (\overline{I}_z^4/S_s) a_w^2 (\overline{\gamma}_{zr}\overline{\beta}_{zr})^4]^{1/3} \mathscr{A}_{sat}^2. \tag{23}$$

Note that in deriving these expressions, we have used $\overline{\beta}_{zr}^2 = 1 - 1/\overline{\gamma}_{zr}^2$, where $\overline{\gamma}_{zr}^2 \approx \gamma_r^2/(1 + \frac{1}{2}a_w^2)$. In a similar manner, one can use the definitions of the normalized quantities to predict estimates for the saturation lengths of different FEL realizations:

$$z_{sat} \approx \gamma_r \overline{\gamma}_{zr}^2 \overline{\beta}_{zr}^3 \mathscr{L} \xi_{sat}, \tag{24}$$

where ξ_{sat} is obtained from Fig. 4, and $\mathscr{L}$ is calculated from Eq. (14).

Within the linear regime, the spatial growth rate is given as

$$\Gamma = \frac{1}{z_{exp}} \approx \frac{1}{\xi_{exp}} \left[\left(\frac{gS_b}{S_s}\right) \left(\frac{\omega}{c}\right)^2 \frac{1}{k_z c^2} \left(\frac{\omega_p^2 a_w^2}{\gamma_r^3 \overline{\gamma}_{zr}^2 \overline{\beta}_{zr}} \right) \right]^{1/3}, \tag{25}$$

where the exponentiation length, $z_{exp} = \gamma_r \overline{\gamma}_{zr}^2 \overline{\beta}_{zr}^3 \mathscr{L} \xi_{exp}$, is consistent with Eq. (24). The growth rate scaling is in agreement with that of previous work.[16] We have found that for amplifier designs, saturation length should not be calculated from the linear growth rate. Instead, it is more appropriate to use the saturation length of Eq. (24). The universal formulation, through the empirical relations in Eq. (19), accounts for the initial transient and eventual saturation (nonlinear) regimes. Saturation lengths based strictly upon linear growth will significantly underestimate the required length.

Of course, there is the issue of whether the interaction is truly noncollective (i.e., Compton). This can be estimated from the ratio of the exponentiation distance to the distance required for a beam plasma oscillation to occur:[9]

$$[(\omega_p/\gamma_r^{3/2}) z_{exp}]/\overline{\beta}_{zr} c = \begin{cases} <1, & \text{Compton} \\ >1, & \text{Raman}, \end{cases} \tag{26}$$

where ω_p is the usual beam plasma frequency, $\omega_p^2 = 4\pi n e^2/m$. Equation (26) can be written as the ratio of the period-averaged beam axial current density $\overline{J}_{bz}$ to the current density J_{coll} at which collective (Raman) effects can no longer be ignored:

$$\overline{J}_{bz} \lesssim J_{coll}, \tag{27a}$$

$$\overline{J}_{bz} = \overline{I}_z(A)/S_b(\text{cm}^2), \tag{27b}$$

$$J_{coll} = [I_A(A)/4\pi](\mathscr{L}^2 \gamma_r^2 \overline{\gamma}_{zr} \overline{\beta}_{zr}^3 \xi_{exp}^2)^{-1}. \tag{27c}$$

Note that the formulas and computations in this work are (strictly speaking) valid only if $\overline{J}_{bz} < J_{coll}$ and when $\overline{\gamma}_{zr} \approx \gamma_r/\sqrt{1 + \frac{1}{2}a_w^2}$.

When determining the collective currents given in Eq. (27c) one can use $\xi_{exp} = 2.4$ since this value is found to be relatively independent of wiggler parameter and injected signal strength. Otherwise, an estimation of z_{exp} can be found from

$$z_{\rm exp} \approx \frac{2z_{\rm sat}}{\ln(P_{\rm sat}/P_0)}, \tag{28}$$

where P_0 is the injected power. Use of Eq. (28) overestimates the exponentiation length and therefore provides a conservative estimate for $J_{\rm coll}$.

IV. TAPERED SECTION

Simplified estimates for the efficiency enhancement achieved with a tapered section can be obtained by manipulations of the unnormalized Eqs. (1)–(3), combined with substitution of the saturated amplitude computed in Eq. (22) of the previous section. Specifically, in the tapered section, we assume that a_w is varied with z so that $d\delta\gamma/dz \approx 0$ for the trapped particles. Another assumption is made that the energy exchange from the beam to the wave is dominated by the trapped particles. Finally, we assume that for the trapped particles the phase bunching function $\langle e^{-i\psi} \rangle$ is approximately constant with z in the tapered region. With these assumptions, Eqs. (1) and (3) are integrated over the length of the tapered section $L_{\rm taper}$ (see Fig. 1). Performing the necessary calculations yields the expression for efficiency

$$\eta_{\rm taper} \approx f_t(\overline{\beta}_{zr}/\beta_{r0})(\Delta\gamma_r/\gamma_{r0} - 1), \tag{29a}$$

$$\Delta\gamma_r = \overline{\gamma}_{zr}\left(\sqrt{1+\tfrac{1}{2}a_{w0}^2} - \sqrt{1+\tfrac{1}{2}a_{wL}^2}\right), \tag{29b}$$

where β_{r0}, γ_{r0} are the values of total (normalized) speed and energy of the electrons at the taper entrance (i.e., at $z = z_{\rm sat}$ in Fig. 1), $a_{w0}(a_{wL})$ is the normalized wiggler potential amplitude at the taper entrance (exit), and f_t is the fraction of trapped particles. Note that this expression is essentially what one might choose based on more phenomenological arguments.

Simplified modeling assumptions yield estimates for other critical parameters in the tapered section. For example, following discussions in Ref. 17, we consider a taper (possibly nonlinear) which is prescribed to keep the quantity

$$\sin\psi_r \equiv \frac{\gamma_r\overline{\beta}_{zr}}{2\mathscr{C}a_w a_s}\left(\frac{c}{\omega}\right)\frac{d\gamma_r}{dz} = \frac{\gamma_{r0}\overline{\beta}_{zr}}{2\mathscr{C}a_w a_{s,\rm sat}}\left(\frac{c}{\omega}\right)\left(\frac{d\gamma_r}{dz}\right)_0 \tag{30}$$

equal to a constant, i.e., equal to its value evaluated at the taper entrance. For such a taper, we can estimate f_t, the trapped fraction, from Fig. 8 of Ref. 17. A conservative linear fit to f_t vs ψ_r in Fig. 8 of Ref. 17 yields

$$f_t \approx 0.8 - (3.2/\pi)\psi_r, \tag{31}$$

where ψ_r is determined from Eq. (30) and $a_{s,\rm sat}$ is found from Eq. (22) given the universal saturated beat wave amplitude $\mathscr{A}_{\rm sat} \approx 0.6$.

In a similar fashion, one can use Eq. (1), setting $d\delta\gamma/dz \approx 0$, to obtain an estimate for the tapered length $L_{\rm taper}$. For example, assuming a linear taper in a_w vs z the result is

$$L_{\rm taper} \equiv \frac{\Delta\gamma_r}{|d\gamma_r/dz|_{z_{\rm sat}}} \approx \frac{\Delta\gamma_r}{2\mathscr{C}a_{w0}a_{s,\rm sat}}\left(\frac{c}{\omega}\right)\gamma_{r0}\overline{\beta}_{zr}. \tag{32}$$

TABLE I. Comparison of estimated values calculated from the universal formulation with values for a 3D simulation of a tapered FEL amplifier at 280 GHz (see Ref. 18).

	Estimate	3D simulation
$P_{\rm sat}$	1.9 GW	1.4 GW
$z_{\rm sat}$	2.6 m	2.2 m
$\overline{J}_{bz}$	...	4600 A/cm^2
$J_{\rm coll}$	820 A/cm^2	...
f_t	0.6	~0.6
$\eta_{\rm taper}$	39%	39%
$L_{\rm taper}$	1.7 m	1.8 m
$P_{\rm out}$	12.9 GW	12.6 GW

Again, $a_{s,\rm sat}$ is obtained from Eq. (22) with $\mathscr{A}_{\rm sat} = 0.6$. Note that the application of Eqs. (31) and (32) to the same tapered section is not necessarily self-consistent. Equations (30) and (31) are relevant to a taper in which ψ_r is kept constant, whereas Eq. (32) applies to a linear taper. Nevertheless, both expressions are expected to provide useful first-order predictions with Eq. (30) tending to overestimate the taper length if nonlinear tapers are employed.

V. DISCUSSION

The utility of the computations and formulas presented in the previous sections will now be discussed. For a benchmark, we consider a high-gain FEL amplifier simulation reported by Chang, Joe, and Scharer.[18] In Table I, the 3D simulation results are compared to predictions from the 1D universal formulation [use of Eqs. (19), (22)–(24), (27)–(32), and Fig. 3]. The agreement is excellent, considering the simplifying assumptions used in the 1D estimates. The modest differences may result from a nonzero detuning and a small, but nonzero, beam thermal spread used in the 3D simulation. Note that the 3D simulation's period-averaged axial current density $\overline{J}_{bz} \approx 4600$ A/cm^2 exceeds the estimated upper limit $J_{\rm coll} \approx 820$ A/cm^2 for Compton behavior. However, this disparity is irrelevant, since the 3D simulation is inherently a high-gain, Compton device due to the neglect of collective effects. Also, note that a typographical error occurs in the stated waveguide dimension of Ref. 18. The waveguide dimensions should read 3.012×3.012 cm^2.[19]

VI. DESIGN OF HIGH-GAIN MILLIMETER-WAVE FEL AMPLIFIER USING A SUPERCONDUCTING SHORT-PERIOD WIGGLER AND SHEET ELECTRON BEAM

The agreement with the results of Ref. 18 demonstrates the utility of using Eqs. (11)–(32) and Figs. 2–4 for first-cut designs of high-gain FEL amplifiers. An important application that may benefit from the use of high-gain FEL amplifiers is the heating of fusion plasmas by high-average power electron-cyclotron resonance heating (ECRH) in the millimeter-wave (mm-wave) regime. In particular, designs for the next generation of high-field, high-density fusion plasma experiments call for ECRH sources to deliver

TABLE II. Designs based upon the universal formulation for a 280- and 560-GHz tapered FEL amplifier with a cw output of 1–2 MW.

Frequency (GHz)	280	560
V_{beam}(MV)	1.0	1.5
I_{beam}(A)	10	10
S_b(cm^2)	0.1×2.0	0.1×2.0
B_{w0}(kG)	10.0	10.0
$B_{w,min}$(kG)	2.0	2.0
l_w (mm)	10.5	10.0
a_{w_0}	0.98	0.93
S_s(cm^2)	0.52×3.0	0.50×3.0
P_{sat} (MW)	0.14	0.14
z_{sat} (m)[a]	0.6	0.9
η_{taper}(%) ($f_t \simeq 0.7$)	17	15
L_{taper}(m)	1.3	2.3
P_{out} (MW)	1.7	2.1

[a]1 kW input for both cases.

one or more megawatts of average power at frequencies between 200 and 600 GHz.[20,21]

Previously, the feasibility of a low- (intrinsic) efficiency FEL oscillator using a short period wiggler ($l_w \lesssim 1$ cm) and a sheet electron beam has been investigated as a possible solution to this need for high average mm-wave power.[22] In this section, we consider the possibilities for an alternative solution: a cw, high-gain, high-efficiency FEL amplifier using a short-period wiggler and a sheet electron beam. The concept is motivated by recent advances in superconducting short-period wiggler design, indicating that values of $a_w \sim 1$ are feasible with wiggler periods of $l_w \lesssim 1$ cm.[23,24]

We have used the universal FEL amplifier results and the procedure discussed in the earlier sections to obtain first-cut designs for high-gain, short-period wiggler FEL amplifiers with a sheet electron beam and a tapered wiggler section for efficiency enhancement. The results are listed in Table II. For beam voltages of approximately 1 MV and beam currents less than 10 A, it is predicted that conventional dc power supplies will soon be available.[22] In these designs we have chosen the minimum peak wiggler field $B_{w,min}$ at 2 kG to ensure sufficient beam focusing[22] at the end of the wiggler. The designs of Table II are applicable for an ECRH source for experimental tokamak plasmas.[20,21] These two designs indicate total lengths of approximately 2–3 m (using a linear taper model) with single-pass intrinsic efficiencies of 15%–20% at cw output powers of 1–2 MW. In all cases the beam current density is well below the collective regime.

As a consequence of the tapered amplifier's higher intrinsic efficiency there are several advantages over the oscillator concept proposed in Ref. 22. The advantages include: (i) roughly one-third the beam power is needed to realize 1 MW of output rf power; (ii) beam focusing is improved due to stronger wiggler fields; and (iii) rf Ohmic heat flux to the waveguide walls is reduced due to lower rf power density in the waveguide. The tradeoffs for these advantages include a much longer interaction length (one order of magnitude) and the (probably) necessary engineering complexity of a cold (4 K) waveguide wall to allow the superconducting magnet coils to get as near to the interaction gap as possible. Both issues underscore the need to keep beam losses to the wall at an extremely low level. Due to the length of the interaction region, this will mean that wiggler field errors must be kept very low to avoid particle diffusion to the walls.[25]

VII. SUMMARY

Using a conveniently normalized set of one-dimensional FEL equations, we have identified several useful "universal" characteristics for high-gain FEL amplifiers with uniform wiggler parameters. Both the normalized exponentiation $\xi_{exp} \approx 2.4$ and the saturated ponderomotive amplitude $\mathscr{A}_{sat} \approx 0.6$ were essentially independent of the injected ponderomotive amplitude $\mathscr{A}_0$. As a result, it was possible to generate a universal expression for the saturated length ξ_{sat} which was only a function of saturated power gain (with a weak, secondary dependence on the wiggler parameter a_w). Unnormalized scaling relations for the saturated radiation power $\mathscr{P}_{sat}$ (using the TE_{01} rectangular mode as an example), and the saturation length z_{sat} were derived in terms of $\mathscr{A}_{sat}$ and ξ_{sat}, respectively. Conditions for neglect of beam space charge were given in terms of the universal parameters. A simple model for a tapered section was also discussed, using an energy balance between wave growth and beam deceleration. This yielded simple, intuitive expressions for efficiency and taper length (the latter based on a linear taper model assumption). The resulting 1D formulas were benchmarked against a 3D numerical simulation of a high-gain, tapered FEL amplifier at 280 GHz. Finally, the results of the theoretical analyses were used to suggest designs for a high-gain mm-wave FEL amplifier using a short-period (superconducting) wiggler and a sheet electron beam. The parameters for this device appear attractive as a high average power mm-wave source for electron cyclotron resonance heating in high-field tokamak plasmas intended as fusion ignition experiments.

ACKNOWLEDGMENTS

The authors wish to acknowledge helpful discussions with Drs. W. M. Fawley, P. E. Latham, A. M. Sessler, and P. Sprangle. Particular gratitude is owed to S.-F. R. Chang for his generous assistance in comparing our formulation to his simulations. This work was supported in part by the U.S. Department of Energy, the Office of Naval Research, a Grainger Faculty Fellowship from the University of Wisconsin, and Presidential Young Investigator Award No. ECS-9057675.

[1] W. B. Colson and J. Blau, Nucl. Instrum. Methods Phys. Res. A **272**, 386 (1988).
[2] A. Serbeto, B. Levush, and T. M. Antonsen, Jr., Phys. Fluids B **1**, 435 (1989).
[3] J. Booske, A. Serbeto, T. M. Antonsen, Jr., and B. Levush, J. Appl. Phys. **65**, 1453 (1989).
[4] T. M. Antonsen, Jr. and B. Levush, Phys. Fluids B **1**, 1097 (1989).
[5] B. Levush and T. M. Antonsen, Jr., Nucl. Instrum. Methods Phys. Res. A **272**, 375 (1988).
[6] T. M. Antonsen, Jr. and B. Levush, Phys. Rev. Lett. **62**, 1488 (1989).
[7] T. M. Antonsen, Jr. and B. Levush, Phys. Fluids B **2**, 2791 (1990).

[8] P. E. Latham, B. Levush, T. M. Antonsen, Jr., and N. Metzler, Phys. Rev. Lett. **66**, 1442 (1991).
[9] P. Sprangle, R. A. Smith, and V. L. Granatstein, in *Infrared and Millimeter Waves*, edited by K. Button (Academic, New York, 1979), Vol. 1, pp. 279–327.
[10] M. Sargent, M. O. Scully, and W. E. Lamb, *Laser Physics* (Addison-Wesley, Reading, MA, 1974), p. 100.
[11] W. B. Colson, IEEE J. Quantum Electron. **QE-17**, 1417 (1981).
[12] T. J. Orzechowski, B. R. Anderson, J. C. Clark, W. M. Fawley, A. C. Paul, D. Prosnitz, E. T. Scharlemann, S. M. Yarema, D. B. Hopkins, A. M. Sessler, and J. S. Wurtele, Phys. Rev. Lett. **57**, 2172 (1986).
[13] N. Metzler, T. M. Antonsen, Jr., and B. Levush, Phys. Fluids B **2**, 1038 (1990).
[14] M. Kumada and A. M. Sessler, "Scaling of the FEL-1D equations," ELF Note 128P, Lawrence Livermore National Laboratory, pp. 1–16, Nov. 25, 1985.
[15] D. J. Radack, J. H. Booske, Y. Carmel, and W. W. Destler, Appl. Phys. Lett. **55**, 2069 (1989).
[16] P.Sprangle and R. A. Smith, Phys. Rev. A **21**, 293 (1980).
[17] N. M. Kroll, P. L. Morton, and M. N. Rosenbluth, IEEE J. Quantum Electron. **QE-17**, 1436 (1981).
[18] S.-F. R. Chang, J. Joe, and J. E. Scharer, IEEE Trans. Plasma Sci. **PS-18**, 451 (1990).
[19] S.-F. R. Chang (private communication).
[20] "ITER Conceptual Design, Interim Report," International Atomic Energy Agency, Vienna, Austria, Oct. 30, 1989.
[21] T. Marshall, J. Lebacqz, and T. Godlove, "Electron Cyclotron Heating—Technology Review," Department of Energy Report, DOE/ER-0366, pp. 1–25, April 1988.
[22] J. H. Booske, D. J. Radack, T. M. Antonsen, Jr., S. W. Bidwell, Y. Carmel, W. W. Destler, H. P. Freund, V. L. Granatstein, P. E. Latham, B. Levush, I. D. Mayergoyz, and A. Serbeto, IEEE Trans. Plasma Sci. **PS-18**, 399 (1990).
[23] See research by P. Walstrom, in FEL'89 Conference Digest, 11th Intl. Conf. on Free Electron Lasers, edited by L. R. Elias and I. Kimel (IEEE, New York, 1989), pp. 100–103.
[24] K. Batchelor, I. Ben-Zvi, R. Fernow, J. Gallardo, H. Kirk, C. Pellegrini, A. Van Steenbergen, and A. Bhowmik, Nucl. Instrum. Methods Phys. Res. A **296**, 239 (1990).
[25] E. Esarey, C. M. Tang, and W. Marable, J. Appl. Phys. **67**, 2210 (1990).